AIP | Applied Physics Letters

Apodized structures for the integration of defect sites into photonic lattices

Martin Boguslawski, Andreas Kelberer, Patrick Rose, and Cornelia Denz

Citation: Applied Physics Letters **105**, 111102 (2014); doi: 10.1063/1.4890099
View online: http://dx.doi.org/10.1063/1.4890099
View Table of Contents: http://scitation.aip.org/content/aip/journal/apl/105/11?ver=pdfcov
Published by the AIP Publishing

Apodized structures for the integration of defect sites into photonic lattices

Martin Boguslawski,[a] Andreas Kelberer, Patrick Rose, and Cornelia Denz
Institut für Angewandte Physik and Center for Nonlinear Science (CeNoS), Westfälische Wilhelms-Universität Münster, 48149 Münster, Germany

(Received 12 March 2014; accepted 25 June 2014; published online 15 September 2014)

We introduce a versatile concept to optically induce photonic structures of local refractive index modulations as well as photonic lattices holding single defect sites. For a given structure, we develop a set of nondiffracting beams obtained by fractionalizing the corresponding spatial spectrum. By combining this set in a multiplexing procedure, we achieve an incoherent combination of all individual structures of the set resulting in a locally addressable refractive index manipulation. We exemplarily present experimental results for apodized, meaning locally confined index changes in a photorefractive crystal resembling a sixfold and a circular symmetric structure. By an additional multiplexing step, we furthermore create periodic photonic lattices featuring embedded defects. [http://dx.doi.org/10.1063/1.4890099]

Breaking symmetries often bears the initiation of additional degrees of freedom and states closely connected with a widening of a system's complexity.[1–3] It is further a global insight that nature's characteristic of breaking symmetry is the fundamental reason for beauty. Thus, naturally occurring lattices in general are hard to find in a perfect, defect-free manner. However, irregularities and defects are the reason for phase transition effects and localization behaviors.[4,5] Especially among photonic crystals and lattices, defect sites allow for propagation and even trapping of light in an otherwise forbidden defect state. These states appear in band gaps between the allowed Bloch mode bands and show intriguing behavior in the linear as well as in the nonlinear regime.[6–8] For instance, defect solitons and stable optical vortices are some of the most astonishing outcomes of particular defect-holding configurations.[9–12]

Various scanning techniques have been developed in recent years to establish defect-holding model systems, such as direct laser writing or holographic lithography.[13,14] Another appropriate candidate is the optical induction of a photonic structure in the refractive index of a nonlinear optical material.[15] In the past, particular shapes of defect manipulated wave fields could be observed in a highly specialized system of photorefractive crystals in experiment.[16]

In combination with the concept of nondiffracting beams (NDBs)[17] as writing light fields, the optical induction technique is highly suitable to generate two-dimensional (2D) photonic structures that are macroscopically elongated in the third dimension. The continuity of the transverse micro-scaled modulation over a macroscopic longitudinal distance thereby is a unique feature among parallel induction techniques and thus allows for an analysis of the propagation along this direction in a fundamental analogy to a temporal development of a probe light field. For such a system, a rather convenient approach is the introduction of a nondiffracting defect beam,[18] as we could show recently. The coherent combination of a hexagonal discrete nondiffracting beam and a π phase-shifted Bessel beam of zeroth order creates a transverse hexagonal intensity distribution with a single suppressed lattice site. Though, for this particular nondiffracting field distribution, the remaining stability of the underlying regular pattern seems to be an exceptional case, as for other configurations the lattice is distorted due to additional interference effects. However, the longitudinal symmetry of a NDB can easily be broken by proper interference with additional light fields. A non-tilted plane wave, for instance, introduces periodic modulation of the overall intensity in the direction of propagation, enabling three-dimensional structuring.[19] To create more complex 2D photonic structures, we introduced the technique of holographic multiplexing.[20,21] Recently, we could show that this technique allows for the generation of multiperiodic structures such as one- and two-dimensional ratchet as well as rectangular superlattices by using NDBs with periodic intensity.[22,23]

In this Letter, we introduce a generally applicable technique to optically induce localized photonic structures of macroscopic elongation. We are going to show as well that these localized structures arising from apodization of a macroscopic structure are the basis for arbitrary photonic patterns holding single defect sites. For both approaches, we apply holographic multiplexing techniques. In the following, we specify the individual steps that are necessary for our multiplexing approach to realize localized photonic structures. For convenience, we conceptualize an effective 2D intensity distribution according to a desired photonic structure. This effective intensity is a result of incoherently superimposing a set of fundamental NDBs adapted from a segmentation procedure of the desired structure's spatial spectrum.

At first, we multiply the 2D field distribution Ψ of a regular NDB with a binary mask M_ρ in the shape of a cylinder function of radius ρ

$$\Psi_\rho = \Psi M_\rho = \mathcal{F}^{-1}[\mathcal{F}(\Psi) * \mathcal{F}(M_\rho)], \tag{1}$$

where * symbolizes a convolution operation. This procedure is illustrated in Fig. 1 from (a) to (b), where the intensity of Ψ_ρ can be identified with (b). From the viewpoint of signal processing, such an apodization operation represents a convolution of the original spatial spectrum with the Fourier transform of the circular aperture [cf. Eq. (1)] which has the shape of the well-known Airy disk. Thus, this multiplication in real space causes a broadening of the original spectral

[a]Electronic mail: martin.boguslawski@uni-muenster.de

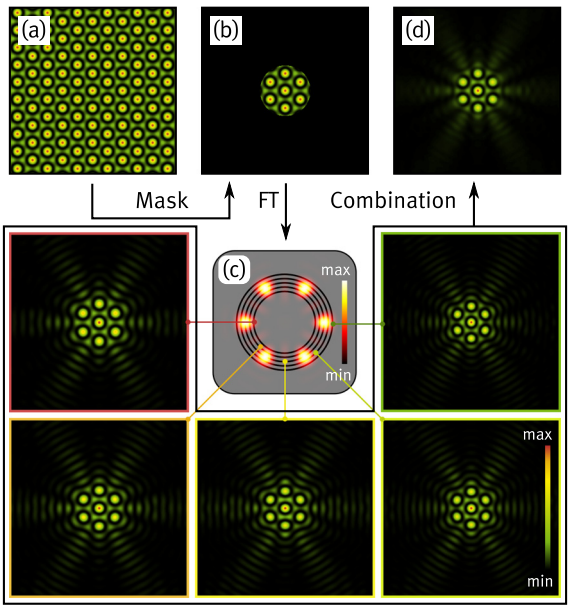

FIG. 1. Schematical illustration of separated spatial spectrum. (a) Original intensity distribution, (b) desired apodized structure, (c) separation of broad spatial spectrum into five spectral rings (highlighted) related to a set of NDBs (Figures arranged around spectrum), (d) resulting effective intensity by combining intensities of deduced set with appropriate weighting factors.

function. Since the spatial frequencies of NDBs are confined on a circle, a spectrum of broad radial width violates the condition for nondiffracting propagation and thus, the desired structure cannot be implemented by a single NDB.

However, to reproduce the desired structure in the manner of an expansion operation, we fractionalize the resulting spectrum into N rings of increasing radius. In Fig. 1(c), the separation is illustrated schematically for the case of $N=5$ by five rings overlaid with the original broadened spectrum. Consequently, each ring resembles the spectrum of a structure acting as one fundamental of the expansion. The fractionalization can be achieved by a multiplication of the broadened spectrum with the spectrum of a Bessel NDB of zeroth order B_0 which is a ring of radius k_t with homogeneous amplitude and phase[17] along the ring

$$\begin{aligned}\psi_i &= \mathcal{F}^{-1}\{\mathcal{F}[\Psi_\rho]\,\mathcal{F}[B_0(k_t^i)]\}\\ &= \Psi_\rho * B_0(k_t^i) \quad \text{with} \quad i=1,\ldots,N. \end{aligned} \tag{2}$$

Hence, we obtain a set of fundamental NDBs ψ_i with $i=1,\ldots,N$, highlighted around the separated spatial spectrum in the center of Fig. 1(c). As shown in Fig. 1(d), the incoherent combination of all ψ_i results in the desired localized structure, provided that the weighting of each contribution is implemented adequately. That is, keeping the maximum and minimum intensities of each ring-like sub spectrum in a fixed mutual amplitude relation. The break up of the phase relation between the individual spatial rings due to our incoherent approach only leads to small contributions of effective intensity not changing the result significantly.

In fact, by incrementing the amount of expansion terms, the original localized structure will be approximated better and better. But already a rather small amount of terms resembles the desired structure in a good agreement, as can be observed by comparing Figs. 1(b) and 1(d). A comparison between the effective intensity in Fig. 1(d) and the intensity of an individual NDB among the set [e.g., lowest middle image in Fig. 1(c)] reveals that prominent side lobes are predominantly suppressed due to apodization using the intensity expansion method.

For an experimental realization, we use an optical setup similar to the one introduced in Ref. 23. The set of NDBs we engineered beforehand can now be applied to optically induce a localized photonic structure. That is, each individual NDB successively illuminates a photosensitive medium for a distinct writing time determined by the mutual weighting of each term. We use liquid crystal spatial light modulators (Holoeye *Pluto* and *LC-R 2500*) to translate computer-calculated phase and amplitude distributions into desired light fields. Thus, for our experiments, we bring laser light of a frequency doubled Nd:YAG laser ($\lambda=532$ nm) to remain nondiffracting within a finite volume.

In the presented experiments, we employ a photorefractive strontium barium niobate (SBN) crystal of $5\times5\times20$ mm^3 which is commonly used to optically induce photonic structures at micro scales.[15,24] In contrast to the transverse dimensions, the propagation distance for a writing beam through the crystal is 20 mm. The crystal's symmetry axis (c-axis) directs along one 5 mm side.

After a complete illumination cycle, the sequence is repeated multiple times until the induced refractive index saturates to the desired level. Notice that the illumination time of each writing beam is much shorter than the typical time constant of several minutes for the used writing intensities to achieve a saturated state of maximum refractive index contrast.[25]

We further implemented a digital holographic analysis method to monitor the refractive index modification, as described in Ref. 23. Using this technique, we obtain the amplitude and phase information of a probe beam that is phase retarded by propagating through the photonic structure. In order to avoid nonlinear self-focusing effects during the analyzing process, we use low-intensity plane wave probe beams. Since the used phase unwrapping algorithms become inaccurate for high index contrasts showing steep gradients that cannot be resolved properly, we exclusively present refractive index distributions for intermediate illumination times of approximately 200 s where the saturation is not yet reached. For such an intermediate state, we estimate a refractive index contrast of approximately $5\text{–}8\times10^{-5}$ where the general saturated contrast is in the range of $1\text{–}3\times10^{-4}$.

To prove the feasibility of the presented method in experiment, we analyze the induction of two exemplary localized structures, namely, a hexagonal arrangement of six local maxima and a doughnut distribution. Both structures originate each from particular NDB intensities where the first one resembles a graphene-like photonic structure[25,26] and the second one is a Bessel beam of first order.

In Fig. 2, results are presented for the hexagonal (a)–(d) as well as for the circular structure (e)–(h). For realizing both structures, we implemented an illumination cycle of $N=6$ multiplexing steps where each cycle takes 10 s. The first column represents the localized structure (highlighted) and the underlying regular intensity distribution (in background). Considering the anisotropic model for a refractive index modulation in a drift dominated photorefractive crystal,[27] we calculated the respective refractive index

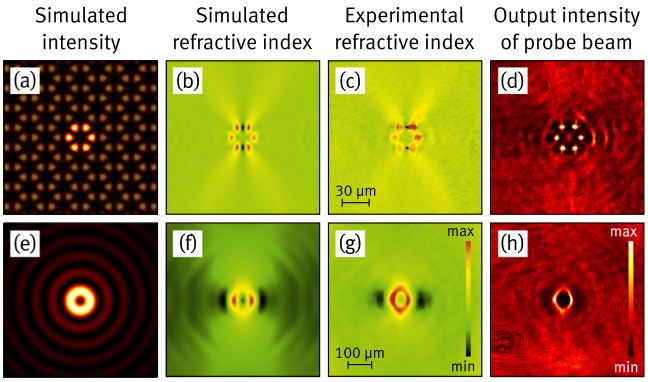

FIG. 2. Localized structure of (a)–(d) sixfold symmetry, (e)–(h) circular symmetry with simulated ((a) and (e)) intensity and ((b) and (f)) refractive index distribution. (c) and (g) Measured refractive index distribution and (d) and (h) intensity of probe beam at output facet. In (a) and (e) underlying regular pattern in background.

distributions [cf. Figs. 2(b) and 2(f)] based on the effective intensities shown in Figs. 2(a) and 2(e).

The experimental distributions for the refractive index averaged over the propagation distance are given in Figs. 2(c) and 2(g). These distributions are extracted from the phase distribution of a plane wave probe beam recorded at the output facet of the induced structure and agree properly with the simulated distributions. Thereby, elliptical rather than circular shapes in Figs. 2(g) and 2(h) are caused by an orientation anisotropy which is characteristic for these kinds of photorefractive crystals.[24,27] Additionally, the related intensity distributions of such a probe beam shown in Figs. 2(d) and 2(h) resemble qualitatively the indicated localized refractive index structures. Notice that these and all following intensity distributions are recorded after an illumination time of approximately 500 s. In contrast to optical induction experiments by a Bessel beam of first order,[24] the characteristic side lobes are predominantly suppressed in the presented case. As a consequence, such an induction configuration allows for fabricating single waveguides with huge elongations of 20 mm even in the linear power regime of a few 100 nW of writing power.

In the following part, we present how to further advance the introduced technique implementing the field switch multiplexing (FSM) method in order to develop defect-holding photonic lattices. To achieve this via the combination of a regular and a localized structure, we introduce an additional illumination step with a regular NDB. We further allow positive and negative external voltages, i.e., static electrical fields directing parallel and anti-parallel to the c-axis. In contrast to a positive voltage effecting a refractive index increase, a local intensity maximum causes a negative change in the refractive index provided that a negative voltage is applied. The sign of the external voltage is often referred to as focusing and defocusing nonlinearity, respectively, since beams show focusing and defocusing characteristics depending on the direction of the field.[28] Exploiting this, we are able to minimize and even invert a refractive index increase when applying a static field of negative amplitude.

In Fig. 3, the development of a periodic hexagonal effective intensity with an embedded seven lattice-site defect via FSM method is presented. Therefore, the formerly

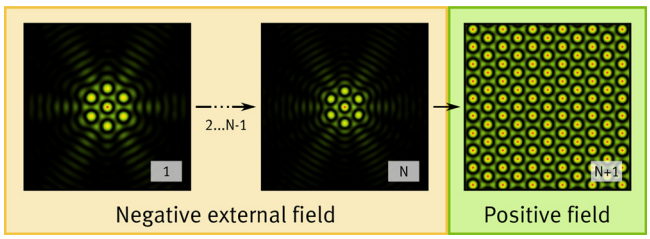

FIG. 3. Schematic of field switch multiplexing for hexagonal defect structure. Yellow frame: N induction steps contributing to localized structure (cf. Fig. 1) with negative external static field. Green frame: additional step with regular pattern and positive external field.

introduced set of intensities involving N induction steps (cf. Fig. 1) is extended by a periodic intensity modulation, increasing the number of contributing intensities to $N+1$. Depending on whether to increase or to decrease the refractive index to a desired contrast level, the proper sign of the external voltage and the particular illumination time have to be chosen.

Experimental results of exemplarily induced photonic defect structures are presented in Fig. 4. Here, two qualitatively different hexagonal lattices are provided with defect sites using the presented FSM method. Correspondingly, the underlying regular refractive index and intensity distribution (respective insets) for these two cases are each shown in Figs. 4(a) and 4(d). In this Figure, (a)–(c) present a single-site defect stemming from a highly negative contribution of the localized part compared to the regular pattern. To experimentally realize this defect structure, we implemented $N+1=11$ multiplexing steps where the illumination times for positive (regular lattice) and negative external field (defect site) during each multiplexing cycle were chosen to be at the ratio of 1:10. The overall duration of each cycle was fixed here to 22 s. For this structure, the symmetry is broken exclusively in the immediate vicinity of the defect site, as the refractive index pattern as well as the probe beam's output intensity in Figs. 4(b) and 4(c) convincingly indicate.

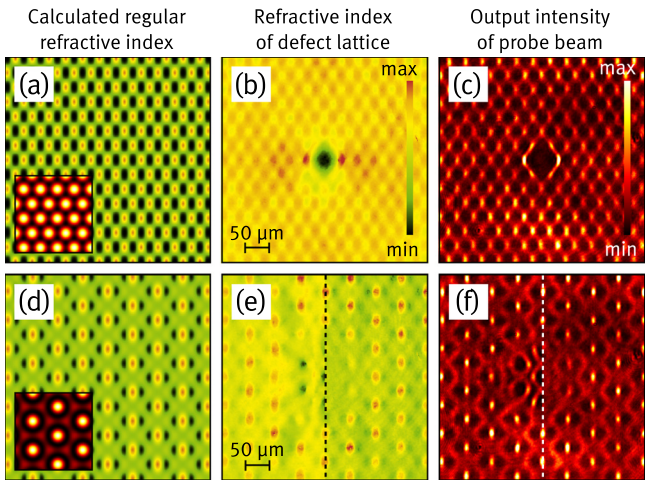

FIG. 4. Hexagonal structure (a)–(c) holding strong negative defect and (d)–(f) advanced hexagonal structure with seven suppressed lattice sites. (a) and (d): Simulated regular refractive index modulation without defect, insets show underlying intensity distribution. (b) and (e): Measured refractive index distributions, (c) and (f): output intensity of plane wave probe beam. In (e) and (f) left and right side show different defect depths due to adapted illumination times.

The results of the induction of a hexagonal structure holding a seven-site defect are shown in Figs. 4(d)–4(f). Here, we implemented $N+1=5$ multiplexing steps. As introduced before, varying the defect strength is feasible by controlling the relation between the illumination times of both the regular lattice and the defect site contribution. This is demonstrated in Figs. 4(e) and 4(f) where the left-part structure is realized due to a ratio of illumination time for regular to defect structure by 5:6 whereas the right-part ratio is 5:2. The respective multiplexing cycle periods were determined to 11 s and 7 s. In particular, the measured refractive index distributions in Fig. 4(e) illustrate the difference, since the defect sites of the left part are suppressed below the regular offset value. In contrast to this, the defect area of the right half is nearly diminished to the offset corresponding to a complete erasure of these individual lattice sites. Against the background of regular band structures, controlling the relative strength of the defect site is an adequate way to regulate the propagation characteristics of defect modes in the linear as well as in the nonlinear regime.[29]

To summarize, we have developed a generally applicable multiplexing technique in order to optically induce 2D apodized photonic structures with a macroscopic elongation in the third dimension. Therefore, we demonstrated that a separation of the spatial spectrum of an individually designed 2D localized structure resulting in a set of NDBs can be used to incrementally multiplex the desired structure into a photorefractive crystal. We further improved this procedure by an additional induction step with a regular pattern in combination with switching the sign of the externally applied voltage. In consequence, implementing such an apodized structure allows to break the symmetry of a regular photonic lattice by combining both. We presented experimental data of optically induced localized as well as defect structures using the introduced incremental multiplexing techniques. In this regard, it should be noted that a three-dimensional defect configuration is possible as well, since the longitudinal symmetry of nondiffracting writing beam propagation can be broken additionally by introducing proper light fields.[19] Hence, our field switch multiplexing technique is a perfect platform for experimental studies on the influence of defect sites in various types and variable amplitude on the propagation behavior of defect modes as well as defect solitons.

[1]P. W. Anderson, Science **177**, 393 (1972).
[2]P. W. Higgs, Phys. Rev. Lett. **13**, 508 (1964).
[3]T. Vicsek, A. Czirók, E. Ben-Jacob, I. Cohen, and O. Sochet, Phys. Rev. Lett. **75**, 1226 (1995).
[4]P. W. Anderson, Phys. Rev. **109**, 1492 (1958).
[5]A. V. Mamaev, M. Saffman, D. Z. Anderson, and A. A. Zozulya, Phys. Rev. A **54**, 870 (1996).
[6]D. R. Smith, S. Schultz, S. L. McCall, and P. M. Platzmann, J. Mod. Opt. **41**, 395 (1994).
[7]W. Królikowski, B. Luther-Davies, and C. Denz, IEEE J. Quantum Electron. **39**, 3 (2003).
[8]N. K. Efremidis and K. Hizanidis, Opt. Express **13**, 10571 (2005).
[9]J. Yang and Z. Chen, Phys. Rev. E **73**, 026609 (2006).
[10]M. J. Ablowitz, B. Ilan, E. Schonbrun, and R. Piestun, Phys. Rev. E **74**, 035601 (2006).
[11]W. H. Chen, X. Zhu, T. W. Wu, and R. H. Li, Opt. Express **18**, 10956 (2010).
[12]D. Song, X. Wang, D. Shuldman, J. Wang, L. Tang, C. Lou, J. Xu, J. Yang, and Z. Chen, Opt. Lett. **35**, 2106 (2010).
[13]J. M. Zeuner, M. C. Rechtsman, R. Keil, F. Dreisow, A. Tünnermann, S. Nolte, and A. Szameit, Opt. Lett. **37**, 533 (2012).
[14]J. Li, Y. Liu, X. Xie, P. Zhang, B. Liang, L. Yan, J. Zhou, G. Kurizki, D. Jacobs, K. S. Wong, and Y. Zhong, Opt. Express **16**, 12899 (2008).
[15]J. W. Fleischer, M. Segev, N. K. Efremidis, and D. N. Christodoulides, Nature **422**, 147 (2003).
[16]I. Makasyuk, Z. Chen, and J. Yang, Phys. Rev. Lett. **96**, 223903 (2006).
[17]J. Durnin, J. J. Miceli, and J. H. Eberly, Phys. Rev. Lett. **58**, 1499 (1987).
[18]A. Kelberer, M. Boguslawski, P. Rose, and C. Denz, Opt. Lett. **37**, 5009 (2012).
[19]J. Becker, P. Rose, M. Boguslawski, and C. Denz, Opt. Express **19**, 9848 (2011).
[20]P. Rose, B. Terhalle, J. Imbrock, and C. Denz, J. Phys. D: Appl. Phys. **41**, 224004 (2008).
[21]Y. Taketomi, J. E. Ford, H. Sasaki, J. Ma, Y. Fainman, and S. H. Lee, Opt. Lett. **16**, 1774 (1991).
[22]M. Boguslawski, A. Kelberer, P. Rose, and C. Denz, Opt. Lett. **37**, 797 (2012).
[23]M. Boguslawski, A. Kelberer, P. Rose, and C. Denz, Opt. Express **20**, 27331 (2012).
[24]P. Rose, M. Boguslawski, and C. Denz, New J. Phys. **14**, 033018 (2012).
[25]P. Rose, T. Richter, B. Terhalle, J. Imbrock, F. Kaiser, and C. Denz, Appl. Phys. B **89**, 521 (2007).
[26]M. Boguslawski, P. Rose, and C. Denz, Phys. Rev. A **84**, 013832 (2011).
[27]A. A. Zozulya and D. Z. Anderson, Phys. Rev. A **51**, 1520 (1995).
[28]W. Królikowski, B. Luther-Davies, C. Denz, J. Petter, C. Weilnau, A. Stepken, and M. Belic, Appl. Phys. B **68**, 975 (1999).
[29]X. Zhu, H. Wang, T.-W. Wu, and L.-X. Zheng, J. Opt. Soc. Am. B **28**, 521 (2011).